



ISSN: 0975-833X

Available online at <http://www.journalcra.com>

International Journal of Current Research  
Vol. 12, Issue, 09, pp.13706-13710, September, 2020

DOI: <https://doi.org/10.24941/ijcr.39574.09.2020>

INTERNATIONAL JOURNAL  
OF CURRENT RESEARCH

## RESEARCHARTICLE

### VIBRATION DETECTION IN PHASE-SENSITIVE OPTICAL TIME DOMAIN REFLECTOMETRY SENSING

Atubga David Atia Ibrahim<sup>1\*</sup>, Bonny Ernestina Linda<sup>3,4</sup>, Edwin Ellis Badu<sup>5</sup>, Harry Akussah<sup>5</sup> and Zinan Wang<sup>1,2</sup>

<sup>1</sup>Key Lab of Optical Fiber Sensing and Communication (Ministry of Education), School of Information and Communication Engineering, University of Electronic Science and Technology of China, Chengdu, China

<sup>2</sup>Center for Information Geoscience, University of Electronic Science, University of Electronic Science and Technology of China, Chengdu, China

<sup>3</sup>School of Management Science and Economics, University of Electronic Science and Technology of China, Chengdu, China

<sup>4</sup>Center for West African Studies (CWAS), University of Electronic Science and Technology of China, Chengdu, China

<sup>5</sup>Department of Information and Communication Studies, University of Ghana-Legon

#### ARTICLE INFO

##### Article History:

Received 15<sup>th</sup> June, 2020

Received in revised form

27<sup>th</sup> July, 2020

Accepted 14<sup>th</sup> August, 2020

Published online 30<sup>th</sup> September, 2020

##### Key Words:

Discrete Wavelet Transform (DWT); Phase-sensitive Optical Time Domain Reflectometry ( $\Phi$ -OTDR); Signal-to-Noise-Ratio (SNR); Hilbert Transform.

#### ABSTRACT

The distributed optical fiber vibration sensors (DOFS) have been widely explored with regards to their significant impact in sensor applications. The Phase-sensitive Optical Time Domain Reflectometry ( $\Phi$ -OTDR) which is known as one of the most vigorous distributed optical fiber sensing technologies has attracted enormous research attention due to its strength in high precision measurements, fast speed response, long perimeter monitoring, as well as vibration detection abilities, among others. However, it becomes very traumatic when data of the said sensing technology meant for vibration detection is obstructed by noise. Therefore, in order to successfully enhance effective vibration detection by the  $\Phi$ -OTDR sensing technology, denoising becomes very essential. The  $\Phi$ -OTDR sensing data therefore was initially processed by Hilbert transform to retrieve both the real and imaginary parts of the complex signal. Then discrete wavelet transform was identified and carefully applied to obtain the desired denoised output of which phase unwrapping was performed to reveal the vibration point. In the experiment, the Signal-Noise-Ratio (SNR) of the location information was greatly improved from 16.0dB to 30.0dB on 2km sensing fiber. Therefore, the proposed method has the potential to precisely extract intrusion location from any harsh setting with strong noise background.

Copyright © 2020, Atubga David Atia Ibrahim et al. This is an open access article distributed under the Creative Commons Attribution License, which permits unrestricted use, distribution, and reproduction in any medium, provided the original work is properly cited.

Citation: Atubga David Atia Ibrahim, Bonny Ernestina Linda, Edwin Ellis Badu, Harry Akussah and Zinan Wang. 2020. "Vibration detection in Phase-sensitive Optical Time Domain Reflectometry Sensing", *International Journal of Current Research*, 12, (09), 13706-13710.

#### INTRODUCTION

The Distributed Optical Fiber Sensing (DOFS) technologies have been keenly explored in recent times of which vibration sensing based on Phase-sensitive Optical Time Domain Reflectometry ( $\Phi$ -OTDR) has widely gained enormous research attention. The said sensing technology has since contributed significantly with respect to fast speed response (Wang, 2016), high sensitivity, large dynamic range sensing and precise location detection, (Peng et al., 2014).

Also, the  $\Phi$ -OTDR sensing technology has equally demonstrated to be proficient, effective and the ultimate in terms of border intrusion monitoring (Chen, 2017). In addition, a reflectometry of 90° optical hybrid has successfully achieved homodyne detection (Wang et al., 2016), whereas the phase information of Rayleigh scattering light wave in an optical fiber similarly demonstrated of transforming a fiber cable into massive sensor array in Distributed Acoustic Sensing (DAS) (Wang, 2019). Additionally, the application of a Single Mode Fiber (SMF) on a truly distributed optical vibration sensor based on  $\Phi$ -OTDR accurately enhanced smooth vibration detection without stress (Lu, 2010). Above all, one key merit of using the  $\Phi$ -OTDR technology in DOFS vibration sensing is that it improves the Signal-To-Noise Ratio (SNR) value in the

\*Corresponding author: Atubga David Atia Ibrahim,

Key Lab of Optical Fiber Sensing and Communication (Ministry of Education), School of Information and Communication Engineering, University of Electronic Science and Technology of China, Chengdu, China.

process of locating an external vibration (Pan, 2011) and (Pang, 2016).

Notwithstanding, vibration detection can only be successfully achieved if the data meant for the said processes is void of noise and other distortions. As a result, a considerable number of signal denoising techniques have been demonstrated including bilateral filtering, bayes-shrink thresholding (Andria, 2013), median filtering (Wang, 2010), Kalman filtering (Jwo, 2010), among others. However, these aforementioned methods come with their intrinsic flaws and not suitable in cases where signals often overlay the noise (Han, 2007) and (Baili, 2009). Per the implications of the foregoing denoising techniques, the strength of each largely depends on the source and kind of data. Although the said techniques might be good for denoising in same sphere, the discrete wavelet transform (DWT) filtering worked perfectly and considered the preferred option. Hence in this paper, the  $\Phi$ -OTDR raw signal was first processed of which the retrieval of the real and the imaginary parts of the signal were obtained by the application of Hilbert transform.

Then DWT was applied to successfully denoise the said signals. Finally, we carried out angle and phase unwrapping to reveal the vibration point. The experimental results by the proposed technique heightened the vibration point with a significant enhancement of the SNR value from 16.0dB to 30.0dB. The next section introduces the DWT approach whereas the proposed method is represented in Section III. Section IV illustrates the experimental setup of the  $\Phi$ -OTDR sensing system with analysis of the results then finally, Section V concludes the paper.

## THE DISCRETE WAVELET TRANSFORM (DWT)

**The discrete wavelet transform denoising approach:** The Discrete Wavelet Transform (DWT) is implemented by the use of discrete sets of wavelet scales and translations to successfully harness effective signal processing while obeying some defined rules. A remarkable fact about the DWT is that it is represented as a mathematical microscope and time-frequency approach used for the analysis of signals after decomposing them over dilated and translated wavelet forms (Lin, 2010). Mathematically, a wavelet is expressed as a function  $\phi$  which belongs to  $L^2(R)$  with a zero (Donoho, 1995), as presented below in equation (1).

$$\int_{-a}^a \phi(t) dt = 0 \quad (1)$$

This process decomposes the signal into an orthogonal set of wavelets components and by thresholding the said components, the denoised signal is obtained. The coefficient is then set to zero if it is smaller than the threshold value. The denoised signal at this point is recovered by performing inverse DWT on the results. Therefore, the wavelet is constructed from a scaling function that describes its scaling features by capturing both the frequency and location information as expressed and presented in equations (2) and (3) respectively;

$$W_{\phi(x_0,y)} = \frac{1}{\sqrt{m}} \sum_n f[n] \phi_{x,y}[n] \text{ for } x \geq x_0 \quad (2)$$

$$W_{\phi(x_0,y)} = \frac{1}{\sqrt{m}} \sum_n f[n] \phi_{x,y}[n] \quad (3)$$

where  $\phi_{x_0,y}[n]$  and  $\phi_{x,y}[n]$  represent the sampled forms of the basic functions  $\phi_{x_0,y}[f]$  and  $\phi_{x,y}[f]$ . In accordance with the inverse form of DWT, it can also be expressed as demonstrated in equation (4) below;

$$\begin{aligned} f[n] &= \frac{1}{\sqrt{m}} \sum_y \omega \phi(x_0,y)[n] \\ &= \frac{1}{\sqrt{m}} \sum_{x=x_0}^x \sum_y \omega \phi(x_0,y) \phi_{x_0,y}[n] \end{aligned} \quad (4)$$

where  $f(n)$ ,  $\phi_{x_0,y}(n)$  and  $\phi_{x,y}(n)$  are considered as discrete functions defined in  $(0, M-1)$ , totally  $M$  points, because the sets  $\{\phi_{x_0,y}[n]\}_{b \in R}$  and  $\{\phi_{x,y}[n]\}_{(x,y) \in R^2, x \geq x_0}$  are orthogonal to each other. Here we can simply take the inner product to obtain the wavelet coefficients as illustrated in equation (2) called the approximation coefficients and in equation (3) expressed as the detailed coefficients. On the other hand, the computational analysis of symlet function  $s\phi$  involving the discrete wavelet transform is presented as follows;

$$\begin{aligned} \phi_{x,y}[n] &= 2^{x/2} \phi[2^x n - y] \\ \sum_n s\phi[n'] &= \sqrt{2} \phi[2(2^x n - y)n'] \end{aligned} \quad (5)$$

Therefore when  $n' = m - 2y$ , then we will have

$$\phi_{x,y}[n] = \sum_m s\phi[m - 2y] \sqrt{2} \phi[2^{x+1}n - m] \quad (6)$$

As a result, if we combine the above equations with equation (2), it becomes;

$$\begin{aligned} w_{\phi}(x,y) &= \frac{1}{\sqrt{m}} \sum_n f[n] \phi_{x,y}[n] \\ &= \frac{1}{\sqrt{m}} \sum_n f[n] 2^{x/2} \phi[2^x n - y] \\ &= \frac{1}{\sqrt{m}} \sum_n f[n] 2^{x/2} \sum_m s\phi[m - 2y] \sqrt{2} \phi[2^{x+1}n - m] \\ &= \sum_m s\phi[m - 2y] \left( \frac{1}{\sqrt{m}} \right) \sum_n f[n] 2^{(x+1)/2} \phi[2^{(x+1)}n - m] \\ &= \sum_m s\phi[m - 2y] w_{\phi}[x+1, m] \\ &= s\phi[-n] * w_{\phi}[x+1, n] \Big|_{n=2y, y \geq 0} \end{aligned} \quad (7)$$

Likewise, the detail coefficients can be expressed as shown below in equation (8)

$$w_{\phi}[x,y] = s_{\phi}[-n] * w_{\phi}[x+1, n] \Big|_{n=2y, y \geq 0} \quad (8)$$

As a result, the original  $\Phi$ -OTDR data in the denoising process can be viewed as approximation coefficients with order  $x$ . That is,  $w_{\phi}[x,y] = w_{\phi}[x,n]$  where by applying equation (7) and (8), the next level of approximation and detail coefficients can be obtained with the desired denoising output. This algorithm is very effective and efficient enough

to find the coefficients, level by level rather than directly using Equations (2) and (3) to find the coefficients.

## THE PRESENTATION OF THE PROPOSED METHOD

**The application of Hilbert transform for retrieving the  $\Phi$ -OTDR complex signal:** To effectively carry out the denoising processes, we applied Hilbert transform for the demodulation of the raw data to first retrieve the complex signal of which further processing for the enhancement of both the real and the imaginary parts of the signal could be obtained by the application of equation (9) as presented below.

$$Q(t) = H[I(t)] \quad (9)$$

Where  $H(I(t))$  represents Hilbert transform and  $Q(t)$  could successfully be retrieved. Hence to efficaciously obtain the real and imaginary parts of the complex signal, we applied equation (10)

$$x = I(t) + jQ(t) \quad (10)$$

of which  $x$  is the complex signal,  $I(t)$  as the real signal and  $Q(t)$  represents the imaginary signal. This was then followed by the denoising processes as presented in the next section.

**The main steps of the proposed denoising technique:** The presentation of the processes involving the discrete wavelet transform denoising and the Hilbert transform approach on the  $\Phi$ -OTDR sensing data for vibration detection is chronologically presented beneath;

- Read the  $\Phi$ -OTDR raw data
- Apply Hilbert Transform for demodulation
- Retrieve complex signal
- Obtain both real and imaginary parts of the signal
- Deploy Discrete Wavelet Transform denoising
- Employ symlet denoising scheme
- Select appropriate decomposition order/level
- Carefully consider the detail wavelet coefficients
- Denoise both the real and imaginary signals
- Perform angle and phase unwrapping algorithm
- Execute differential phase trace and extraction
- Carry out vibration detection processes
- Evaluate and calculate for the SNR value
- Further compute for the SNR enhancement value
- Finally evaluate and end the processes.

Consequently, after successfully obtaining the desired denoised signals with significantly preserved details, the next section was duly executed for the extraction and vibration detection as discussed beneath.

**The process of vibration extraction and detection:** In order to successfully achieve the vibration detection, the raw forms of both the real and imaginary signals were retrieved by the application of equation (10) as discussed in the preceding stages. Then we applied equations (7) - (8) to enhance the desired denoised signals. These denoised real and imaginary signals were then converted into the magnitude or phase format to facilitate the extraction processes for the vibration detection by applying equation (11) below.

$$a(t) = \sqrt{x^2(t) + H^2[x(t)]} \quad (11)$$

Further, we perform angle ( $\angle$ ) and phase unwrapping to successfully extract the vibration point along the sensing signal, as expressed in equation (12) below;

$$\phi(t) = \text{unwrapping}[\angle(I(t) + Q(t))] \quad (12)$$

Where  $I(t)$  and  $Q(t)$  represent both the denoised forms of the real and imaginary signals respectively, of which the angle and phase unwrapping was successfully applied to harness the retrieval of  $\phi(t)$  for the phase trace. Therefore the angle and phase unwrapping processes finally heightened the vibration detection of the  $\Phi$ -OTDR sensing signal with its corresponding statistical features.

## THE $\Phi$ -OTDR EXPERIMENTAL SETUP AND DISCUSSIONS OF RESULTS

**The experimental setup of the  $\Phi$ -OTDR system:** The experimental setup of the  $\Phi$ -OTDR system is demonstrated with an ultra-narrow-line width (100Hz) laser operating at 1550 nm employed as the light source with a 1:99 Polarization Maintaining (PM) coupler. The laser output is divided into two branches by a 1:99 PM coupler forming a probe light and a local reference light. One of the branches is modulated by an In-phase/ Quadrature (I/Q) modulator with 500MHz frequency shift to generate the pulsed probe wave (with 100ns pulse width, allowing for 10m spatial resolution). The sampling rate is 2GHz and that of the repetition rate of the probe pulse is 50kHz. The probe pulse is injected into the sensing fiber through a circulator and the Rayleigh Scattering (RS) signal is introduced into a 90° hybrid. The 1% branch of the laser output is used as the LO. Then before the LO is injected into hybrid, a Polarization Controller (PC) is inserted in order to match the LO with the selected polarization branch of the hybrid. The two outputs of the hybrid are converted into electrical signals by two ports AC coupled detector and then sampled by the OSC. At the position of 2km, a 12.7m bare fiber is coiled over a cylindrical PZT, used as the test point. The process of phase unwrapping algorithm, signal reconstruction leading to denoising and vibration detection are completed in real-time by a personal computer involving the application MATLAB processing environment as presented in Figure 1.

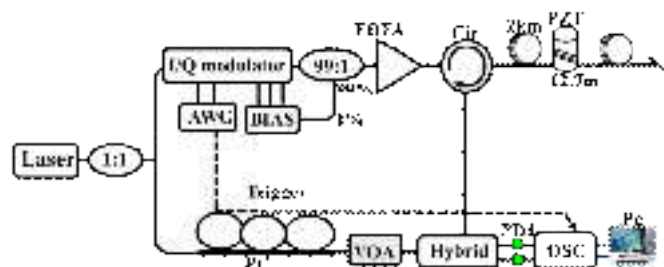


Figure 1. The experimental setup of the hybrid  $\Phi$ -OTDR sensing system for vibration detection. IQ: In-phase Quadrature Modulator; EDFA: Erbium-Doped Fiber Amplifier; VOA: Variable Optical Attenuator; PC: Polarization Controller; PD: Photo Detector; PZT: Piezo Transducer, Pc: Personal computer

**Analysis of and discussions of the denoised results:** As previously stated, the retrieval of the complex signal of the

$\Phi$ -OTDR was performed by applying Hilbert Transform of which both the real and imaginary signals were successfully achieved by the application of equations (9) and (10) respectively. The DWT denoising technique was therein carried out by applying equations (7) and (8) accordingly. The desired denoised real and imaginary signals were then obtained. Hence, the results of the real original and its denoised signals are demonstrated in Figure 2(a) and Figure 2(b) respectively. Comparatively, there exist relatively vast difference in terms of the noise levels per the denoised signal and its corresponding original signal. The intensity of a distance at approximately 2100m onwards on the denoised signal shown in Figure 2(b) has significantly presents much reduced noise level as compared to that of the exhibit of the corresponding original figure as presented in Figure 2(a) below.

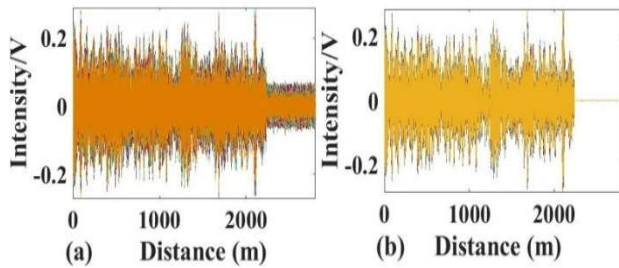


Figure 2. Original and denoised real signal

The representation of the imaginary part and its denoised signal are equally illustrated in Figure 3(a) and Figure 3(b) respectively as shown below. Constructively, it is apparent that there is much reduction of the noise level per the intensity of a distance at approximately 2100m on both figures states in the preceding.

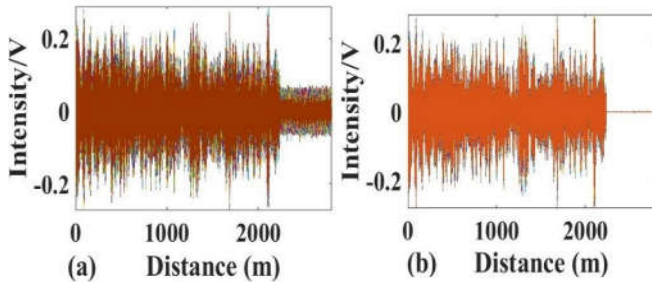


Figure 3. Imaginary and denoised imaginary signal

**Phase trace extraction for vibration detection:** In the DOFS vibration detection involving the  $\Phi$ -OTDR sensing technology, a Piezoelectric Transducer (PZT) with the maximum vibration frequency response of 50kHz is used as the vibration actuator during the experimental stage.

A single vibration is added to the position of 2110m along the sensing fiber. Several traces in the  $\Phi$ -OTDR system were recorded by a double channel oscilloscope. The extraction of the phase trace to detect the vibration was then executed soon after obtaining the denoised real and imaginary signals where we performed angle and phase unwrapping by the application of equations (11) and (12) respectively. The reflection of the traces on the signal appeared to be very serrated due to the presence of much interference and fading thereby leading to the existence of extreme fading points on the original signal as presented in Figure 4(a).

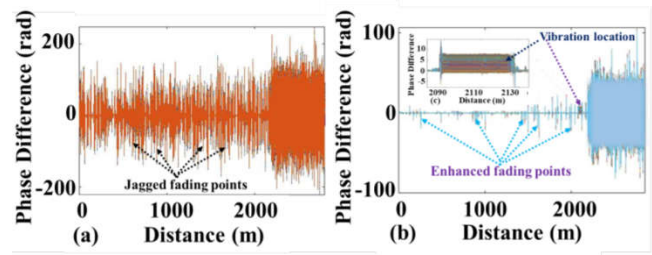


Figure 4. Original and denoised phase trace

In contrast, Figure 4(b) clearly demonstrate the vibration point detected with improved fading points at a distance of approximately 2110m and equally presents a closed view of the said point. In the history of optical imaging and wireless telecommunication as well as signal denoising, fading has been a serious phenomenon such that the phase extraction on the differential phase traces sometimes becomes very difficult to precisely locate the vibration zone after denoising. Nonetheless, the proposed method has successfully enhanced the denoised signals and aided smooth extraction of the vibration zone per the normalized denoised intensity phase trace as revealed in Figure 4(b). The depiction of the original time domain signal and its denoised form are also presented in Figure 5. The red irregular line represents the original data clearly demonstrating the level of extreme noise present while the blue thin line therein indicates its denoised form as illustrated below in Figure 5(a) and Figure 5(b) respectively.

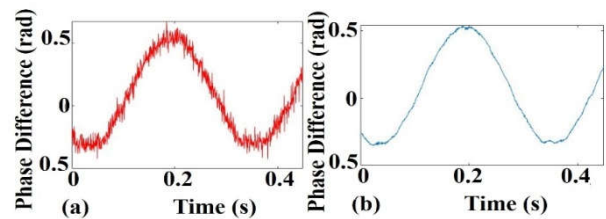


Figure 5. Original and denoised time domain signals

The SNR value was then calculated with respect to the time domain signal by the application of equation (13) as presented beneath.

$$SNR = 10 \log_{10} \left( \frac{S_{power}}{N_{power}} \right) \quad (13)$$

where  $S_{power}$  refers the signal power and  $N_{power}$  also representing the power of the noise. We therefore obtained the SNR value from 16.0 dB to 30.0 dB corresponding to both the original and denoised signals. To successfully reaffirm the SNR enhancement level, we further carried out standard deviation ( $\sigma$ ) computation per the said vibration point by applying equations (14) and (15) correspondingly as presented below.

$$\sigma = \sqrt{\text{var}(p - q)} \quad (14)$$

where  $p$  represents the noisy signal and  $q$  also signifying the cleaned signal. We obtained 0.4670 and 0.0934 as the values of the standard deviation corresponding to the original signal and the denoised signal respectively.

$$\Delta SNR = 10 \log_{10} \left( \frac{\sigma^2_{Original\ signal}}{\sigma^2_{Denoised\ signal}} \right) \quad (15)$$

The proof of the SNR enhancement was finally confirmed by the application of equation (15). Then a final value of 14.0 dB was achieved as the improved SNR value.

## Conclusion

In this paper, we successfully demonstrate the proposed method on  $\Phi$ -OTDR sensing data for vibration detection. It considerably reduced the noise with preserved significant details that aided smooth extraction and detection of the vibration point. There was equally an improvement of the SNR value. The technique proved effective and could withstanding real time performance in distributed  $\Phi$ -OTDR vibration detection and could equally be replicated in other related DOFS sensing technologies for similar tasks. In conclusion, the proposed technique has the potential to precisely extract intrusion location from any harsh sensing domain with strong noise background.

## Acknowledgment

This work is supported by Sichuan Youth Science and Technology Foundation (2016JQ0034).

## REFERENCES

- Andria, G. Attivissimo F, Lanzolla AML, Savino M. "A suitable threshold for speckle reduction in ultrasound images". IEEE Transactions on Instrumentation and Measurement. 2013;62(8):2270-9.
- Baili, J. Lahouar S, Hergli M, Al-Qadi IL, Besbes K. "GPR signal de-noising by discrete wavelet transform". NDT E Int. 2009;42(8):696-703.
- Chen, D. Liu QW, He Z. "Phase-detection distributed fiber-optic vibration sensor without fading-noise based on time-gated digital OFDR". Optics Express. 2017;25(7):8315-25.
- Donoho D. L, Johnstone IM, Kerkycharian G, Picard D. Wavelet shrinkage: Asymptopia? J Roy Statist Soc. 1995;57:301369.
- Han, M. Liu Y, Xi J, Guo W. "Noise smoothing for nonlinear time series using wavelet soft threshold", IEEE Signal Process Letter. 2007;14(1):62-5.
- Jwo D. J, Cho TS. "Critical remarks on the linearised and extended Kalman filters with geodetic navigation examples". Measurement. 2010;43(9):1077- 89.
- Lin, C. Liu A. Tutorial of the Wavelet Transform. 2010.
- Lu, Y. Zhu T, Chen LA, Bao XY. "Distributed vibration sensor based on coherent detection of phase-OTDR". Lightw Technol. 2010;28(22):3243- 9.
- Pan, Z. Liang K, Ye Q, Cai H, Qu R, Fang Z. "Phase-sensitive OTDR system based on digital coherent detection". Asia Communications and Photonics Conference and Exhibition, (Optical Society of America). 2011;83110S.
- Pang, F. He M, Liu H, Mei X, Tao J, Zhang T, *et al.* "A fading-discrimination method for distributed vibration sensor using coherent detection of  $\Phi$ -OTDR". IEEE Photonics Technology. 2016;28(23):2752-5.
- Peng, F. Wu H, Jia XH, Rao YJ, Wang ZN, Peng ZP. "Ultra-long high sensitivity  $\Phi$ -OTDR for high spatial resolution intrusion detection of pipelines". Optics Express. 2014;22(11):13804-10.
- Wang G. H, Li DH, Pan WM, Zang ZX. "Modified switching median filter for impulse noise removal". Signal Process. 2010;90(12):3213-8.
- Wang, P. Lou S, Liang S, Zhang Y. "Selective average based threshold algorithm for  $\Phi$ -OTDR distributed fiber-optic sensing system". Infrared Laser Engineering. 2016;45(3).
- Wang, Z. Zhang L, Wang S, Xue N, Peng F, Fan M, *et al.* "Coherent  $\Phi$ -OTDR based on IQ demodulation and homodyne detection". Optics Express. 2016;24(2):853-8.
- Wang, Z. Zhang B, Xiong J, Fu Y, Lin S, Jiang J, *et al.* "Distributed acoustic sensing based on pulse-coding phase sensitive OTDR", IEEE Internet of Things. 2019;6(4):6117-24.

\*\*\*\*\*